

Opposing modulation of Cx26 gap junctions and hemichannels by CO₂

Sarbjit Nijjar¹, Daniel Maddison¹, Louise Meigh¹, Elizabeth de Wolf¹, Thomas Rodgers², Martin Cann³, Nicholas Dale^{1*}

¹School of Life Sciences
University of Warwick
Coventry
CV4 7AL

²School of Chemical Engineering and Analytical Science
University of Manchester
Oxford Road
Manchester
M13 9PL

³Department of Biosciences
Durham University
Stockton Road
Durham
DH1 3LE

* N.E.Dale@warwick.ac.uk

Running title: CO₂-dependent modulation of Cx26 gap junctions

Key words: Connexin; cell coupling; hemichannel; gap junction

ToC Category: Molecular and Cellular

This paper was first published as preprint: Nijjar, S., Maddison, D., Meigh, L., de Wolf, E., Rodgers, T., Cann, M. and Dale, N. (2019) Opposing modulation of Cx26 gap junctions and hemichannels by CO₂. **bioRxiv** doi.org/10.1101/584722

Key points

- A moderate increase in PCO₂ (55 mmHg) closes Cx26 gap junctions.
- This effect of CO₂ is independent of changes in intra- or extracellular pH.
- The CO₂ dependent closing effect depends on the same residues (K125 and R104) that are required for the CO₂-dependent opening of Cx26 hemichannels.
- Pathological mutations of Cx26 abolish the CO₂-dependent closing of the gap junction
- Elastic network modelling suggests that the effect of CO₂ on Cx26 hemichannels and gap junctions is mediated through changes in the lowest entropy-state of the protein.

Summary

Cx26 hemichannels open in response to moderate elevations of CO₂ (PCO₂ 55 mmHg) via a carbamylation reaction that depends on residues K125 and R104. Here we investigate the action of CO₂ on Cx26 gap junctions. Using a dye transfer assay, we found that an elevated PCO₂ of 55 mmHg greatly delayed the permeation of a fluorescent glucose analogue (NBDG) between HeLa cells coupled by Cx26 gap junctions. However, the mutations K125R or R104A abolished this effect of CO₂. Whole cell recordings demonstrated that elevated CO₂ reduced the Cx26 gap junction conductance (median reduction 5.6 nS, 95% confidence interval, 3.2 to 11.9 nS) but had no effect on Cx26^{K125R} or Cx31 gap junctions. CO₂ can cause intracellular acidification, but using 30 mM propionate we found that acidification in the absence of a change in PCO₂ caused a median reduction in the gap junction conductance of 5.3 nS (2.8 to 8.3 nS). This effect of propionate was unaffected by the K125R mutation (median reduction 7.7 nS, 4.1 to 11.0 nS). pH-dependent and CO₂-dependent closure of the gap junction are thus mechanistically independent. Mutations of Cx26 associated with the Keratitis Ichthyosis Deafness syndrome (N14K, A40V and A88V) also abolished the CO₂-dependent gap junction closure. Elastic network modelling suggests that the lowest entropy state when CO₂ is bound, is the closed configuration for the gap junction but the open state for the hemichannel. The opposing actions of CO₂ on Cx26 gap junctions and hemichannels thus depend on the same residues and presumed carbamylation reaction.

Introduction

The canonical function of connexins is to form intercellular junctions between cells –gap junctions – through the docking of hexameric connexons in the opposing membrane of each cell. However, the individual connexons –known as hemichannels –can also function on their own (Stout *et al.*, 2004; Weissman *et al.*, 2004; Pearson *et al.*, 2005; Huckstepp *et al.*, 2010b). Hemichannels act as plasma membrane channels, which in addition to mediating transmembrane ionic currents, also permit the

transmembrane fluxes of small molecules such as ATP (Stout *et al.*, 2002; Pearson *et al.*, 2005; Kang *et al.*, 2008; Huckstepp *et al.*, 2010a).

We have studied the hemichannels of connexin26 (Cx26) and found that these hemichannels are directly gated by CO₂ (Huckstepp *et al.*, 2010a; Meigh *et al.*, 2013; Meigh *et al.*, 2014). CO₂ opens the hemichannel and permits the efflux of ATP, which can act as a neurotransmitter. This is particularly important in the CO₂ sensitive control of breathing where Cx26 hemichannels in the medulla oblongata act as novel chemosensory transducers (Huckstepp *et al.*, 2010a; Huckstepp & Dale, 2011). Cx26 hemichannels also impart CO₂ sensitivity to dopaminergic neurons of the substantia nigra and GABAergic neurons of the ventral tegmental area (Hill *et al.*, 2020). The action of CO₂ on Cx26 has been proposed to occur via carbamylation of the residue K125. The carbamylated lysine forms a salt bridge to R104 of the neighbouring subunit. These intersubunit carbamate bridges bias the hemichannel to the open configuration (Meigh *et al.*, 2013). Extensive evidence supports a direct action of CO₂ on the hemichannel rather than an indirect effect via pH: 1) in isolated inside-out or outside-out patches changes in PCO₂ at constant pH alter Cx26-gating (Huckstepp *et al.*, 2010a); 2) insertion of the carbamylation motif into Cx31, which is insensitive to CO₂, creates mutant Cx31 hemichannels that can be opened by CO₂ (Meigh *et al.*, 2013); 3) mutation of the key residues K125 and R104 to respectively arginine and alanine destroys CO₂-sensitivity of the hemichannel; 4) the mutations K125E and R104E (in effect engineering the action of CO₂ into the subunit via the carboxy group of glutamate) create constitutively open hemichannels which are CO₂-insensitive (Meigh *et al.*, 2013); 5) the mutation K125C creates a hemichannel that can be opened with NO or NO₂ via a nitrosylation reaction on the cysteine residue at 125 and subsequent salt bridge formation to R104 (Meigh *et al.*, 2015); and 6) the double mutation K125C and R104C creates a redox-sensitive hemichannel presumably via disulfide bridge formation between the cysteine residues at 104 and 125 (Meigh *et al.*, 2015).

Although the actions of CO₂ on Cx26 hemichannels are well characterized, we have not studied the action of CO₂ on Cx26 gap junctions. When the two connexons dock to form a complete gap junction, there is likely to be significant conformational rearrangement and constraint of the resulting dodecameric complex. Therefore, we cannot assume that CO₂ will modulate a complete gap junction in the same way as a hemichannel. There has been a previous study on the closing effect of CO₂ on Cx32 and Cx26 gap junctions expressed in *Xenopus* oocytes (Young & Peracchia, 2004). This prior study used non-physiological conditions in which both the extracellular and intracellular pH would become very acidic: exposure to 30-100% CO₂ in the absence of bicarbonate in the extracellular medium. This study most likely reported an effect of pH on the gap junction. In this paper, we report the actions of much lower physiological concentrations of CO₂ (~9%), in a CO₂/HCO₃⁻ buffered system at constant extracellular pH, on gap junctions formed between pairs of

HeLa cells expressing Cx26. We find that modest increases in PCO_2 *close* complete gap junctions, and that this is most likely a direct effect mediated through its binding to the same residues that result in the *opening* of the hemichannel. This result reinforces the need to develop further high-resolution structures for Cx26 hemichannels and gap junctions with and without CO_2 bound.

Methods

HeLa cell culture and transfection

HeLa DH (ECACC) cells were grown in DMEM supplemented with 10% fetal bovine serum, 50 µg/mL penicillin/streptomycin and 3 mM CaCl₂. For electrophysiology and intercellular dye transfer experiments, cells were seeded onto coverslips in 6 well plates at a density of 2x10⁴ cells per well. After 24 hrs the cells were transiently transfected with Cx26 constructs tagged at the C-terminus with a fluorescent marker (mCherry) according to the GeneJuice Transfection Reagent protocol (Merck Millipore). The HeLa cells stably expressing mouse Cx26 were originally obtained from Dr K. Willecke (Elfgang *et al.*, 1995).

Cx26 mutants

The mutations used in this study were introduced into the Cx26 gene by QuikChange site directed mutagenesis and have been described previously (Meigh *et al.*, 2013) (Cook *et al.*, 2019).

Solutions used

Standard aCSF: 124 mM NaCl, 3 mM KCl, 2 mM CaCl₂, 26 mM NaHCO₃, 1.25 mM NaH₂PO₄, 1 mM MgSO₄, 10 mM D-glucose saturated with 95% O₂/5% CO₂, pH 7.5, PCO₂ 35 mmHg.

Hypercapnic aCSF: 100 mM NaCl, 3 mM KCl, 2 mM CaCl₂, 50 mM NaHCO₃, 1.25 mM NaH₂PO₄, 1 mM MgSO₄, 10 mM D-glucose, saturated with 9% CO₂ (with the balance being O₂) to give a pH of 7.5 and a PCO₂ of 55 mmHg respectively.

Propionate solution: 82mM NaCl, 30 mM Na-propionate, 3 mM KCl, 2 mM CaCl₂, 26 mM NaHCO₃, 1.25 mM NaH₂PO₄, 1 mM MgSO₄, 10 mM D-glucose saturated with 95% O₂/5% CO₂, pH 7.5, PCO₂ 35 mmHg.

Imaging assay of gap junction transfer

2-Deoxy-2-[(7-nitro-2,1,3-benzoxadiazol-4-yl)amino]-D-glucose, NBDG, was included at 200 µM in the patch recording fluid, which contained: K-gluconate 130 mM; KCl 10 mM; EGTA 5 mM; CaCl₂ 2 mM, HEPES 10 mM, pH was adjusted to 7.3 with KOH and a resulting final osmolarity of 295 mOsm. Cells were imaged on a Cleverscope (MCI Neuroscience) with a Photometrics Prime camera under the control of Micromanager 1.4 software. LED illumination (Cairn Research) and an image splitter (Optosplit, Cairn Research) allowed simultaneous imaging of the mCherry tagged Cx26 subunits and the diffusion of the NBDG into and between cells. Coupled cells for intercellular dye transfer experiments were initially selected on the basis of tagged Cx26 protein expression and the presence

of a gap junctional plaque, easily visible as a band of mCherry fluorescence (e.g. Figures 1 and 2). After establishing the whole cell mode of recording, images were collected every 10 seconds.

Patch Clamp recordings from coupled cells

Cover slips containing non-confluent cells were placed into a perfusion chamber at room temperature in sterile filtered standard aCSF. Two Axopatch 200B amplifiers were used to make whole-cell recordings from pairs of HeLa cells. The intracellular fluid in the patch pipettes contained: K-gluconate 130 mM, KCl 10 mM, EGTA 10 mM, CaCl₂ 2 mM, HEPES 10 mM, sterile filtered, pH adjusted to 7.3 with KOH. An agarose salt bridge was used to avoid solution changes altering the potential of the Ag/AgCl reference electrode. All whole-cell recordings were performed at a holding potential of -50 mV. Steps to -40 mV were applied to each cell in alternation to measure the whole cell and gap junction conductances. The current flow from the cell at -40 mV to the cell at -50 mV flows through the gap junction and can thus be used to calculate the gap junction conductance. The outward current during the +10 mV step in each cell represents the whole cell conductance which is a combination of all current pathways out of the cell. These comprise any intrinsic conductances and also the gap junction conductance itself.

Elastic network modelling

Elastic network model (ENM) simulations were performed based on the regular implementation using PDB file 2ZW3, where all the C α atoms in the protein within a given cut-off radius (8 Å) were joined with simple Hookean springs (Tirion, 1996; Rodgers *et al.*, 2013a). The spring constants were set to a constant value of 1 kcal mol⁻¹ Å⁻². The presence of CO₂ was represented in the ENM by the inclusion of an additional Hookean spring between residues K125 and R104 of each set of neighbouring monomers, following the same procedure previously used for ligand binding (Rodgers *et al.*, 2013b). The mass-weighted second derivatives of this potential energy matrix were diagonalised to produce eigenvectors, e , which are the normal modes, and eigenvalues which are the squares of the associated frequencies, ω , and can be used to calculate the free energy of each mode.

The first six modes, that is the lowest frequency modes, represent the solid body translational and rotational motions of the protein and are thus excluded from the analysis. The overlap of the modes in the unbound and CO₂ bound states were calculated by comparison of the eigenvectors (Rodgers *et al.*, 2013a). A value of 1 indicates that the motions are identical whereas a value of 0 indicates that the motions are completely different.

Statistics and Reproducibility

Statistical analysis was performed with the R language. Data has been plotted as box and whisker plots, with individual points superimposed, where the box is interquartile range, bar is median, and whisker extends to most extreme data point that is no more than 1.5 times the interquartile range. Each individual point is from a single patch clamp experiment and is counted as a replicate. Statistical comparisons were performed with the Kruskal Wallis test (for multiple comparisons) or Mann Whitney U test. Exact p values are shown for comparisons that showed a significant difference between samples.

Results

Rate of dye transfer between coupled cells shows CO₂-dependence of Cx26 gap junctions

Many investigators have used dye transfer assays to demonstrate the presence of gap junctions (Spray *et al.*, 1991; Elfgang *et al.*, 1995; Abbaci *et al.*, 2007). We therefore adapted this type of assay to test whether increases in PCO₂ could alter the permeation of a fluorescent glucose analogue (2-Deoxy-2-[(7-nitro-2,1,3-benzoxadiazol-4-yl)amino]-D-glucose, NBDG) through Cx26 gap junctions formed between HeLa cells. Starting with HeLa cells that stably expressed untagged Cx26, we made whole cell recordings from a single cell in a coupled pair. After introducing NBDG, via the patch pipette, into one of the cells (the *donor*) of a coupled pair, we recorded the time taken for the dye to diffuse into the coupled (*acceptor*) cell and achieve 10% of the fluorescence intensity of the donor cell (Figure 1A). If the gap junction is sensitive to CO₂, then permeation of NBDG from the donor to acceptor cell should be altered by elevated PCO₂ (Figure 1A). By recording from pairs of HeLa cells that stably expressed Cx26, we found that NBDG, rapidly permeated into coupled cells in solutions with a PCO₂ of 35 mmHg (Figure 1C). When the recording was initiated in a saline with a PCO₂ of 55 mmHg, there was little permeation during the period of high PCO₂ and this only occurred once the PCO₂ was reduced to 35 mmHg (Figure 1C). We refined this assay by performing it on cells that had been transfected with Cx26 tagged with mCherry. This allowed us to directly visualize the gap junctions and thus select pairs of coupled cells for the assay (Figure 1B). Once again, we found that the level of PCO₂ altered the time it took for NBDG to permeate from the donor to the acceptor cell (Figure 1B, C).

Having established the validity of the fluorescence assay to detect CO₂-sensitive intercellular coupling, we next investigated whether the CO₂-sensitivity of Cx26 gap junctions depended on the same residues (K125 and R104) that are necessary for the CO₂-sensitivity of the Cx26 hemichannel (Meigh *et al.*, 2013). We examined the effect of two mutations K125R and R104A that individually remove CO₂ sensitivity from the hemichannel. Cx26^{K125R} and Cx26^{R104A} formed gap junctions

between HeLa cells (Figure 2A) that were readily permeated by NBDG. Our data showed that unlike wild type Cx26 gap junctions, CO₂ made no difference to the rate of dye transfer between cells coupled via Cx26^{K125R} or Cx26^{R104A} (Figure 2A, B). CO₂-dependent gap junction closure appears to require the same residues that are essential for hemichannel opening.

Electrical coupling via Cx26 gap junctions is sensitive to CO₂

To confirm the observations made during intercellular dye transfer assays, we made simultaneous whole cell recordings from isolated pairs of Cx26-expressing HeLa cells that were in close apposition, as these cells had a high probability of being electrically coupled. On establishing whole cell recordings from each cell, the cells were clamped at a holding potential of -50 mV. We used a simple protocol of repeated 10 mV steps, alternating in each cell (see Methods). In all the illustrations, the downward currents during the voltage steps are proportional to the junctional conductance. Untransfected parental HeLa cells could exhibit gap junction coupling but this was insensitive to CO₂ (median change in conductance -0.03 nS, 95% confidence limits -0.2 and 0.11, *n*=10; Figure 3A, B). In cells that stably expressed mouse Cx26, application of hypercapnic saline (PCO₂ 55 mmHg) at a constant extracellular pH of 7.5 caused a reduction of junctional coupling (Figure 3A, B). In some cases, this was a partial effect and, in other cases, the coupling between cells was completely abolished. Overall the median change of the gap junction conductance (from control to 55 mmHg PCO₂) was -5.6 nS (95% confidence limits -11.9 and -3.2 nS, *n*=29).

We next tested the requirement for the carbamylation motif for gap junction closure by CO₂ in the electrophysiological assay. Gap junctions formed between HeLa cells expressing Cx26^{K125R} were insensitive to a PCO₂ of 55 mmHg (Figures 3A, B; median change in conductance 0.01 nS, 95% confidence limits 0.2 and -0.06 nS, *n*=14). Furthermore, gap junctions of Cx31, which lacks the carbamylation motif (Meigh *et al.*, 2013), were also insensitive to a PCO₂ of 55 mmHg (Figure 3A, B; median change in conductance 0.07 nS, 95% confidence limits 0.44 and -0.29 nS, *n*=11).

We have therefore used two independent methods to demonstrate that Cx26 gap junctions are closed by moderate changes in CO₂ (a PCO₂ of 55 mmHg) and this CO₂-dependent closure depends upon the same residues (K125 and R104) that are required for hemichannel opening by CO₂.

CO₂-dependent and pH-dependent closure of Cx26 gap junctions can be dissociated by the K125R mutation

A possible mechanism by which CO₂ could close the gap junction is via intracellular acidification. CO₂ is known to permeate membranes and, by combining with water, can acidify the intracellular

milieu. In prior studies, very high levels of CO₂ (30-100%) have been used as a pharmacological method to close a variety of gap junctions (Spray *et al.*, 1991; Young & Peracchia, 2004). We therefore tested whether intracellular acidification, imposed independently of CO₂ by application of 30 mM propionate (Jahromi *et al.*, 2002; Haussig *et al.*, 2008), could close the Cx26 gap junction, and whether this could be altered by the K125R mutation, which eliminates CO₂-dependent closure. This level of propionic acid will cause far greater intracellular acidification than that caused by the elevated CO₂ used in this study (Cook *et al.*, 2012). Propionic acid treatment reduced the gap junction conductance of wild type Cx26 by 5.3 nS (median, 95% confidence limits 2.8 and 8.3 nS, *n*=12, Figure 4). This manipulation also reduced the gap junction conductance of Cx26^{K125R} by a similar amount 7.7 nS (median, 95% confidence limits 4.1 and 11.0 nS, *n*=13, Figure 4). The actions of CO₂ and intracellular pH on the Cx26 gap junction conductance are thus of similar magnitude, but mechanistically independent. Specifically, pH-induced gap junction closure does not require K125, whereas CO₂-dependent closure does require this residue. This in turn suggests that CO₂ has a direct action on Cx26, most probably via the carbamylation reaction that we have proposed for the opening of hemichannels (Meigh *et al.*, 2013), to cause closing of the gap junction.

Effect of KID syndrome mutations on CO₂-dependence of gap junction coupling

We have previously shown that KID syndrome mutations A88V, N14K, and A40V (Figure 5) abolish the ability of CO₂ to open the mutant hemichannels (Meigh *et al.*, 2014; de Wolf *et al.*, 2016; Cook *et al.*, 2019). Recently, we discovered that certain KID syndrome mutations induce alternative splicing of the Cx26 mutation when this is tagged with a fluorescent protein (Cook *et al.*, 2019). This splicing results in poor expression and cell death but can be prevented by also mutating the 5' splice site (Cook *et al.*, 2019). However, the 5' splice site cannot be silently mutated so we chose a conservative mutation, M151L (Figure 5), which appeared to have little effect on Cx26 expression by itself. Cx26^{M151L} hemichannels are blocked normally by extracellular Ca²⁺ and they retain CO₂-sensitivity (Cook *et al.*, 2019). Furthermore, Cx26^{A40V,M151L} hemichannels are insensitive to CO₂ (Cook *et al.*, 2019).

When the M151L mutation was combined with the KIDS mutations, A40V, A88V or N14K (Figure 5), in each case, the doubly mutated Cx26 was invariably capable of forming functional gap junctions through which NBDG could permeate (Figure 6). For all three mutations, the Cx26 gap junction remained open in the presence of 55 mmHg PCO₂ (Figure 6), a concentration that would normally close the wild type gap junction (Figures 1-3). Thus, the KIDS mutations not only prevent CO₂-dependent opening of the hemichannel, but also prevent CO₂-dependent closing of the gap junction, at least when combined with M151L. Interestingly, the effect of N14K on hemichannel sensitivity to CO₂ is less than the other KIDS mutations (de Wolf *et al.*, 2016) and this parallels the trend in our

data that permeation of NBDG through the Cx26^{N14K,M151L} gap junctions, while still occurring, may be slightly slowed at the higher level of PCO₂ (Figure 6C, D).

As the mutation M151L is a rare allele associated with non-syndromic hearing loss (Siemering *et al.*, 2006), we tested whether this mutation by itself affected gap junctions. Cx26^{M151L} permitted gap junction formation as gap junction plaques were clearly visible between expressing cells (Figure 7A). However, in 47 different recordings we did not observe either dye coupling (Figure 7B) or the electrophysiological hallmarks of electrical coupling (slowed capacitive charging currents during a voltage step indicative of current flow through the gap junction). By contrast, cells expressing Cx26^{A40V,M151L}, Cx26^{A88V,M151L} and Cx26^{N14K,M151L} exhibited dye coupling in 14/15, 12/12 and 12/12 recordings respectively. These frequencies of coupling are statistically different $\chi^2 = 82.2$ (3 degrees of freedom, $p=5.1 \times 10^{-18}$). We conclude that the mutation M151L prevents permeation through gap junctions that are apparently formed but either remain closed at the transjunctional potential studied here, or are otherwise non-functional. This finding implies that the KIDS mutations appear to compensate for the deficiency in gap junction permeability introduced by the M151L mutation.

Elastic network modelling

Previous experimental data points to the importance of carbamylation of K125 and the formation of a salt bridge to R104 in the adjacent subunit to facilitate Cx26 hemichannel opening in response to CO₂. It is not clear from this mechanism alone why the dodecameric Cx26 gap junction would be closed by CO₂. Previous work has used coarse-grained modelling to demonstrate a mechanism whereby CO₂ constrains the Cx26 hemichannel in the open state (Meigh *et al.*, 2013). We therefore used further coarse-grained modelling to probe the difference in behaviour of the Cx26 hemichannel and gap junction. Coarse-grained modelling reduces protein atomistic complexity for efficient computational studies of harmonic protein dynamics and is particularly suited to examining the contribution of entropy to channel opening over millisecond time scales (Sherwood *et al.*, 2008). While it is not possible to be certain that such calculated dynamics are true in the absence of experimentally determined structures, coarse-grained modelling has helped to support and explain structural data for membrane protein conformational changes (Shrivastava & Bahar, 2006; Sherwood *et al.*, 2008; Zheng & Auerbach, 2011; Isin *et al.*, 2012).

In an Elastic Network Model (ENM) the C α -atom coordinates of an atomic resolution structure are used to represent a protein structure. Global protein harmonic motions within the ENM consists of a defined number of modes, each of a characteristic frequency and representing a particular harmonic motion within the protein. ENMs reproduce protein global low frequency modes well in comparison

to experimental data (Delarue & Sanejouand, 2002; Valadie *et al.*, 2003). We therefore built coarse-grained ENMs (Tirion, 1996) to gain insight into the mechanism by which CO₂ maintains the Cx26 hemichannel in the open state but the Cx26 gap junction in the closed state. ENMs were constructed using the coordinates from high-resolution crystal structures for the Cx26 hemichannel and gap junction in the CO₂ unbound state. CO₂ was represented in the ENMs by the inclusion of additional Hookean springs between residues K125 and R104 of neighbouring monomers in both the hemichannel and the gap junction (Meigh *et al.*, 2013).

We examined the similarities between eigenvectors for the Cx26 hemichannel and gap junction to understand the changes in harmonic protein motion caused by CO₂-binding. The main open-close mode in the Cx26 hemichannel is defined as the lowest frequency mode that ignores the solid body translational and rotational motions. The solid body translational and rotational motions consist of six modes and so the open-close mode is mode 7 (Meigh *et al.*, 2013). This open-close mode in the hemichannel in the absence of CO₂ (mode 7) becomes reordered as mode 15 in the presence of CO₂ (Figure 8A; red-bordered square). The main open-close mode in the gap junction in the absence of CO₂ (mode 10; modes 7-9 represent motions between the two hexamer rings) becomes reordered as mode 24 in the presence of CO₂ (Figure 8B; green-bordered square). Analysis of the overlap between the main open-close mode in the gap junction and hemichannel in the absence of CO₂ reveals an almost complete overlap between mode of the hemichannel (mode 7) and the gap junction (mode 10) (Figure 8C, blue-bordered square). The basic open-close dynamics are therefore likely similar between gap junction and hemichannel.

To understand the differing roles of CO₂ in the hemichannel and gap junction, we calculated a range of partially open and closed eigenvectors for both the hemichannel and the gap junction. We then calculated at each state, for both the hemichannel and gap junction, the free energy for CO₂-binding and the influence of CO₂ on the open/close eigenvector. This calculation provides a free energy for each state examined along the open/close eigenvector. Calculation of the free energy difference between the CO₂-bound and unbound state provides information on the stability (binding energy of CO₂ needed) for each state. In this case, the closer the value is to zero, the less energy needed to bind CO₂ (Figure 8D). The x-axis of the Figure represents trajectory along the open/close eigenvector where the higher the value the more closed the hemichannel or gap junction. The y-axis of the Figure represents the difference in free energy for the CO₂-bound and non-bound state where the higher the value is hypothesised to be less preferable for CO₂-binding. On binding CO₂, the hemichannel (6mer) or gap junction (12mer) will progress along the open/close eigenvector to make the difference in free energy more favourable for the CO₂-bound state.

For the hemichannel, it is energetically favourable to bind CO₂ in the open-state and then energetically unfavourable to close. For the gap junction it is energetically favourable to bind CO₂ in the closed state and then energetically unfavourable to open. The differences in the open/closed state of the gap junction and hemichannel in response to CO₂ can therefore be explained through entropy contributions to free energy change.

Discussion

The key result from our study is that Cx26 gap junctions are closed by a direct action of CO₂ on the protein. Our prior publications have demonstrated the opening action of CO₂ on Cx26 hemichannels (Huckstepp *et al.*, 2010a; Meigh *et al.*, 2013; Meigh *et al.*, 2014; de Wolf *et al.*, 2016; de Wolf *et al.*, 2017; Cook *et al.*, 2019; Dospinescu *et al.*, 2019). This paper further shows that these diametrically opposite actions of CO₂ on gap junctions and hemichannels depend on the same residues and presumably the same carbamate bridging mechanism.

Opposing modulation of gap junctions and hemichannels has been reported before. LPS and bFGF inhibit Cx43 gap junctions and open Cx43 hemichannels. While apparently similar to the results reported in this study, the modulation of these two entities is downstream of kinase activity and the signaling actions of arachidonate metabolites; i.e. these are indirect effects on Cx43 and are unlikely to involve the same residues in the protein (De Vuyst *et al.*, 2007). Similarly, the cytokines IL1 β and TNF α also inhibit Cx43 gap junctions and open Cx43 hemichannels (Retamal *et al.*, 2007a). Both of these effects are mediated through a p38 MAPK dependent pathway. However, hemichannel opening triggered by these cytokines is sensitive to inhibition of nitric oxide synthase or changing redox state (Retamal *et al.*, 2007b), whereas the gap junction closure is insensitive to redox state. Thus, for the two entities, the mechanisms of modulation evoked by the p38 MAPK pathway differ (Retamal *et al.*, 2007a).

Independence of pH- and CO₂-dependent modulation of Cx26 gap junctions

A possible alternative interpretation of our data is that CO₂ caused intracellular acidification and thus closed the gap junction. Under this interpretation, CO₂ would have no direct action on Cx26. This interpretation is unlikely for two reasons. Firstly, only modest increases in PCO₂ around the physiological norm were required to close Cx26 gap junctions. Such changes will only cause modest intracellular acidification. By contrast very profound acidification to pH values below 6.5 is required to close the Cx26 gap junction channel (Khan *et al.*, 2020). Secondly, and more importantly, the mutation K125R prevents the CO₂-dependent closure of the gap junction, but does not affect the closing effect of acidification induced by application of propionate (Figure 4). The action of CO₂ and

pH on the gap junction are therefore mechanistically independent at the moderate levels of CO₂ used in this study. This independence of mechanistic action of pH and CO₂ is also true for Cx26 hemichannels as acidification causes hemichannel closure (Yu *et al.*, 2007), whereas a modest increase in PCO₂ causes hemichannel opening (Huckstepp *et al.*, 2010a; Meigh *et al.*, 2013; de Wolf *et al.*, 2017; Cook *et al.*, 2019; Hill *et al.*, 2020).

Although the carbamylation motif in Cx26 is required for both the CO₂-dependent opening of hemichannels and the CO₂-dependent closure of gap junctions, the link between the CO₂-dependent modulation of hemichannels and gap junctions is not immutable. Cx26 hemichannels of the lung fish *Lepidosiren* are insensitive to CO₂ owing to the presence of an extended C-terminus, yet their gap junctions are still closed by CO₂ (Dospinescu *et al.*, 2019). The contrary case is demonstrated by Cx32: hemichannels of this connexin can be opened by CO₂, but Cx32 gap junctions are insensitive to the same doses of CO₂ (Dospinescu *et al.*, 2019).

Implications for structural biology of Cx26

The crystal structure of Cx26 shows the molecule in the form of a gap junction (Maeda *et al.*, 2009). The two connexons dock via interactions involving the two extracellular loops (E1 and E2) of each subunit. There are multiple hydrogen bonds formed between the opposing E1 and E2 loops of each connexon (Maeda *et al.*, 2009). These give a tight interaction that is likely to alter and constrain the conformation of hemichannels docked in a gap junction versus undocked hemichannels. The opposing modulation of gap junctions and hemichannels by CO₂ must presumably arise from the conformational differences between free versus docked hemichannels.

Our ENM calculations of the interaction of CO₂ with Cx26 hemichannels used the docked hemichannel from the gap junction as a model for the structure of the free hemichannel (Meigh *et al.*, 2013). This model allowed us to propose a plausible gating mechanism for CO₂-dependent opening of the hemichannel, which we have supported with extensive mutational analysis (Meigh *et al.*, 2013). We exploited this knowledge to introduce novel gating mechanisms via the same intersubunit interactions by mutating Lys125 to Cys (Meigh *et al.*, 2015). This made the hemichannel NO-sensitive, via nitrosylation of the Cys125 and interaction with Arg104 of the neighbouring subunit. The double mutation -K125C, R104C - made the hemichannel redox sensitive (via redox modulation of disulfide bridges between subunits) (Meigh *et al.*, 2015). The mutated residues in these Cx26 variants are some considerable distance apart –far further than the short distances normally required for the ionic and covalent interactions between the respective residues. That these mutations were nevertheless effective at changing the gating of Cx26 implies considerable flexibility of the hemichannel that can bring apparently distant residues close enough to interact (Meigh *et al.*, 2015).

Despite this success in using a half gap junction as a model for the free hemichannel, the results in this study suggest the need for considerable caution in any future structural modeling of hemichannels. Not only may the isolated hemichannel be far more flexible than a hemichannel that is part of a gap junction, but it may also have a substantially different conformation. New structures of Cx26 hemichannels and gap junctions are therefore needed to probe their conformational differences, and provide firm mechanistic understanding of the differential modulation of hemichannels and gap junctions by CO₂.

KIDS mutations and Cx26 gap junctions

There are relatively few reports of the effects of KIDS mutations on Cx26 gap junctions. Prior reports suggest that the A40V mutation prevents Cx26 gap junction formation (Montgomery *et al.*, 2004). Clearly our data suggest that, in HeLa cells and in combination with the mutation M151L at least, the A40V mutation does not prevent formation of functional gap junctions (Figure 6a). Our data suggests further that N14K and A88V KIDS mutations (once again in combination with M151L) do not prevent gap junction formation and that these gap junctions are highly permeable to NBDG.

KIDS mutations are thought to cause the syndrome through gain-of-function. Several lines of evidence suggest that KIDS mutated Cx26 hemichannels are leaky: either they are less sensitive to Ca²⁺ blockade (Sanchez *et al.*, 2010; Mese *et al.*, 2011; Lopez *et al.*, 2013; Zhang & Hao, 2013; Sanchez *et al.*, 2014) or have an altered voltage sensitivity such that they spend more time in the open state at transmembrane potentials closer to the resting potential (Sanchez *et al.*, 2016; Valdez Capuccino *et al.*, 2019). Our finding that three KIDS mutations studied here prevent gap junctions from closing to CO₂ is effectively a further gain of function caused by these mutations: they will remain open under conditions of elevated CO₂. Interestingly, A40V hemichannels in oocytes are less sensitive to pH blockade than wild type Cx26 hemichannels, indicating that this mutation has multiple effects on the gating of these channels (Sanchez *et al.*, 2014). It is also interesting that the three KIDS mutations tested here could compensate for the loss of gap junction coupling induced by M151L. This observation is suggestive that these mutations enhance channel permeation and are also consistent with the gain-of-function hypothesis.

Although not a KIDS mutation, M151L has been reported to be associated with deafness (Siemering *et al.*, 2006). Our finding that it prevents functional gap junction communication suggests possible underlying mechanistic cause of hearing loss with this mutation. The endocochlear potential is essential for hearing -it provides the driving force for K⁺ to enter the hair cells through the mechanosensory ion channels present in their stereocilia. Cx26 gap junctions are a pathway for

diffusion of K⁺ between the fibrocytes, basal cells and intermediate cells of the stria vascularis (Wangemann, 2006) and have been proposed to form part of the pathway that recycles K⁺ away from the hair cells and back into the endolymph, although this has been disputed (Zhao, 2017). Genetic deletion of Cx26 reduces the endocochlear potential by about half (Chen *et al.*, 2014). Given that M151L prevents gap junction coupling (although not the formation of gap junctions *per se*), we predict that it would reduce the endocochlear potential and that this is the reason for hearing impairment.

Physiological implications

As Cx26 exists both as gap junctions and hemichannels, our findings have substantial physiological significance. In the context of breathing, Cx26 hemichannels are important and we have already explored their significance for chemosensory control (Huckstepp *et al.*, 2010b). However, there are reports of gap junctions in various nuclei implicated in the control of breathing (Dean *et al.*, 2002; Solomon *et al.*, 2003). CO₂-dependent uncoupling of Cx26 gap junctions between cells may therefore be an additional mechanism that contributes to chemosensory control.

In lungfish and amphibia, hemichannels of Cx26 are insensitive to CO₂ despite possessing the carbamylation motif (Dospinescu *et al.*, 2019). The extended C-terminal tail of Cx26 in these species interferes with hemichannel opening. However, the Cx26 gap junctions of these species can still be closed by CO₂ (Dospinescu *et al.*, 2019). The ancestral function of the carbamylation motif in Cx26 was therefore most likely to close the gap junction and the new function of hemichannel opening only arose in the amniotes (Dospinescu *et al.*, 2019). Given that it has been conserved over many hundreds of millions of years, the CO₂-dependent closure of Cx26 gap junctions must have some important physiological function. What this may be remains open to question, but we speculate that if a single cell in a coupled network were to be excessively metabolically active, it would act as a sink for metabolites such as ATP, glucose or lactate from the coupled cells. As the metabolically active cell would produce more CO₂ this could be a self-regulating mechanism to preserve network integrity by uncoupling the “run-away” cell from the network thereby reducing its drain on the communal pool of metabolites. It is interesting in this context, that the PCO₂ of renal cortex and liver (respectively 57 and 64 mmHg), two organs where Cx26 and Cx32 are abundantly expressed, is considerably higher than the PCO₂ of systemic circulation (39-45 mmHg) (Hogg *et al.*, 1984).

Acknowledgements

We thank the MRC (MR/P010393/1) (ND) and BBSRC (BB/S015132/1) (MC) for support. ND is a Royal Society Wolfson Research Merit Award Holder.

Author contributions

SN, DM, ND: Acquisition and analysis of data

LM, EdW: Generation of mutants and stable cell lines

TR, MC: Elastic network modelling

ND wrote the paper, all authors commented on the final version.

Conflict of Interest Statement

The authors declare that they have no conflicts of interest.

Data availability

All data generated or analysed during this study are included in this published article.

References

- Abbaci M, Barberi-Heyob M, Stines JR, Blondel W, Dumas D, Guillemin F & Didelon J. (2007). Gap junctional intercellular communication capacity by gap-FRAP technique: a comparative study. *Biotechnology journal* **2**, 50-61.
- Chen J, Chen J, Zhu Y, Liang C & Zhao HB. (2014). Deafness induced by Connexin 26 (GJB2) deficiency is not determined by endocochlear potential (EP) reduction but is associated with cochlear developmental disorders. *Biochem Biophys Res Commun* **448**, 28-32.
- Cook J, de Wolf E & Dale N. (2019). Cx26 keratitis ichthyosis deafness syndrome mutations trigger alternative splicing of Cx26 to prevent expression and cause toxicity in vitro. *Royal Society open science* **6**, 191128.
- Cook ZC, Gray MA & Cann MJ. (2012). Elevated Carbon Dioxide Blunts Mammalian cAMP Signaling Dependent on Inositol 1,4,5-Triphosphate Receptor-mediated Ca²⁺ Release. *Journal of Biological Chemistry* **287**, 26291-26301.
- De Vuyst E, Decrock E, De Bock M, Yamasaki H, Naus CC, Evans WH & Leybaert L. (2007). Connexin hemichannels and gap junction channels are differentially influenced by lipopolysaccharide and basic fibroblast growth factor. *Mol Biol Cell* **18**, 34-46.
- de Wolf E, Cook J & Dale N. (2017). Evolutionary adaptation of the sensitivity of connexin26 hemichannels to CO₂. *Proc R Soc B* **284**: **20162723**.
- de Wolf E, van de Wiel J, Cook J & Dale N. (2016). Altered CO₂ sensitivity of connexin26 mutant hemichannels in vitro. *Physiol Rep* **4**, e13038.
- Dean JB, Ballantyne D, Cardone DL, Erlichman JS & Solomon IC. (2002). Role of gap junctions in CO₂ chemoreception and respiratory control. *Am J Physiol Lung Cell Mol Physiol* **283**, L665-670.

- Delarue M & Sanejouand YH. (2002). Simplified normal mode analysis of conformational transitions in DNA-dependent polymerases: the elastic network model. *J Mol Biol* **320**, 1011-1024.
- Dospinescu V-M, Nijjar S, Spanos F, Cook J, de Wolf E, Biscotti MA, Gerdol M & Dale N. (2019). Structural determinants of CO₂-sensitivity in the β connexin family suggested by evolutionary analysis. *Communications Biology* **2**, 331.
- Elfngang C, Eckert R, Lichtenberg-Fraté H, Butterweck A, Traub O, Klein RA, Hülser DF & Willecke K. (1995). Specific permeability and selective formation of gap junction channels in connexin-transfected HeLa cells. *J Cell Biol* **129**, 805-817.
- Haussig S, Schubert A, Mohr FW & Dhein S. (2008). Sub-chronic nicotine exposure induces intercellular communication failure and differential down-regulation of connexins in cultured human endothelial cells. *Atherosclerosis* **196**, 210-218.
- Hill E, Dale N & Wall MJ. (2020). Moderate changes in CO₂ modulate the firing of neurons in the VTA and substantia nigra. *iScience*, 101343.
- Hogg RJ, Pucacco LR, Carter NW, Laptook AR & Kokko JP. (1984). In situ PCO₂ in the renal cortex, liver, muscle, and brain of the New Zealand white rabbit. *Am J Physiol* **247**, F491-498.
- Huckstepp RT & Dale N. (2011). Redefining the components of central CO₂ chemosensitivity--towards a better understanding of mechanism. *J Physiol* **589**, 5561-5579.
- Huckstepp RT, Eason R, Sachdev A & Dale N. (2010a). CO₂-dependent opening of connexin 26 and related beta connexins. *J Physiol* **588**, 3921-3931.
- Huckstepp RT, id Bihi R, Eason R, Spyer KM, Dicke N, Willecke K, Marina N, Gourine AV & Dale N. (2010b). Connexin hemichannel-mediated CO₂-dependent release of ATP in the medulla oblongata contributes to central respiratory chemosensitivity. *J Physiol* **588**, 3901-3920.
- Isin B, Tirupula KC, Oltvai ZN, Klein-Seetharaman J & Bahar I. (2012). Identification of motions in membrane proteins by elastic network models and their experimental validation. *Methods Mol Biol* **914**, 285-317.
- Jahromi SS, Wentlandt K, Piran S & Carlen PL. (2002). Anticonvulsant actions of gap junctional blockers in an in vitro seizure model. *J Neurophysiol* **88**, 1893-1902.
- Kang J, Kang N, Lovatt D, Torres A, Zhao Z, Lin J & Nedergaard M. (2008). Connexin 43 hemichannels are permeable to ATP. *J Neurosci* **28**, 4702-4711.
- Khan AK, Jagielnicki M, McIntire WE, Purdy MD, Dharmarajan V, Griffin PR & Yeager M. (2020). A Steric "Ball-and-Chain" Mechanism for pH-Mediated Regulation of Gap Junction Channels. *Cell Rep* **31**, 107482.
- Lopez W, Gonzalez J, Liu Y, Harris AL & Contreras JE. (2013). Insights on the mechanisms of Ca²⁺ regulation of connexin26 hemichannels revealed by human pathogenic mutations (D50N/Y). *J Gen Physiol* **142**, 23-35.
- Maeda S, Nakagawa S, Suga M, Yamashita E, Oshima A, Fujiyoshi Y & Tsukihara T. (2009). Structure of the connexin 26 gap junction channel at 3.5 Å resolution. *Nature* **458**, 597-602.

- Meigh L, Cook D, Zhang J & Dale N. (2015). Rational design of new NO and redox sensitivity into connexin26 hemichannels. *Open Biol* **5**, 140208.
- Meigh L, Greenhalgh SA, Rodgers TL, Cann MJ, Roper DI & Dale N. (2013). CO₂ directly modulates connexin 26 by formation of carbamate bridges between subunits. *eLife* **2**, e01213.
- Meigh L, Hussain N, Mulkey DK & Dale N. (2014). Connexin26 hemichannels with a mutation that causes KID syndrome in humans lack sensitivity to CO₂. *eLife* **3**, e04249.
- Mese G, Sellitto C, Li L, Wang HZ, Valiunas V, Richard G, Brink PR & White TW. (2011). The Cx26-G45E mutation displays increased hemichannel activity in a mouse model of the lethal form of keratitis-ichthyosis-deafness syndrome. *Mol Biol Cell* **22**, 4776-4786.
- Montgomery JR, White TW, Martin BL, Turner ML & Holland SM. (2004). A novel connexin 26 gene mutation associated with features of the keratitis-ichthyosis-deafness syndrome and the follicular occlusion triad. *Journal of the American Academy of Dermatology* **51**, 377-382.
- Pearson RA, Dale N, Llaudet E & Mobbs P. (2005). ATP released via gap junction hemichannels from the pigment epithelium regulates neural retinal progenitor proliferation. *Neuron* **46**, 731-744.
- Retamal MA, Froger N, Palacios-Prado N, Ezan P, Sáez PJ, Sáez JC & Giaume C. (2007a). Cx43 Hemichannels and Gap Junction Channels in Astrocytes Are Regulated Oppositely by Proinflammatory Cytokines Released from Activated Microglia. *The Journal of Neuroscience* **27**, 13781-13792.
- Retamal MA, Schalper KA, Shoji KF, Bennett MV & Saez JC. (2007b). Opening of connexin 43 hemichannels is increased by lowering intracellular redox potential. *Proc Natl Acad Sci U S A* **104**, 8322-8327.
- Rodgers TL, Burnell D, Townsend PD, Pohl E, Cann MJ, Wilson MR & McLeish TC. (2013a). $\Delta\Delta$ PT: a comprehensive toolbox for the analysis of protein motion. *BMC Bioinformatics* **14**, 183.
- Rodgers TL, Townsend PD, Burnell D, Jones ML, Richards SA, McLeish TC, Pohl E, Wilson MR & Cann MJ. (2013b). Modulation of Global Low-Frequency Motions Underlies Allosteric Regulation: Demonstration in CRP/FNR Family Transcription Factors. *PLoS Biol* **11**, e1001651.
- Sanchez HA, Bienkowski R, Slavi N, Srinivas M & Verselis VK. (2014). Altered Inhibition of Cx26 Hemichannels by pH and Zn²⁺ in the A40V Mutation Associated with Keratitis-Ichthyosis-Deafness Syndrome. *J Biol Chem* **289**, 21519-21532.
- Sanchez HA, Mese G, Srinivas M, White TW & Verselis VK. (2010). Differentially altered Ca²⁺ regulation and Ca²⁺ permeability in Cx26 hemichannels formed by the A40V and G45E mutations that cause keratitis ichthyosis deafness syndrome. *J Gen Physiol* **136**, 47-62.
- Sanchez HA, Slavi N, Srinivas M & Verselis VK. (2016). Syndromic deafness mutations at Asn 14 differentially alter the open stability of Cx26 hemichannels. *J Gen Physiol* **148**, 25-42.
- Sherwood P, Brooks BR & Sansom MS. (2008). Multiscale methods for macromolecular simulations. *Current opinion in structural biology* **18**, 630-640.

- Shrivastava IH & Bahar I. (2006). Common mechanism of pore opening shared by five different potassium channels. *Biophys J* **90**, 3929-3940.
- Siemering K, Manji SS, Hutchison WM, Du Sart D, Phelan D & Dahl HH. (2006). Detection of mutations in genes associated with hearing loss using a microarray-based approach. *J Mol Diagn* **8**, 483-489; quiz 528.
- Solomon IC, Chon KH & Rodriguez MN. (2003). Blockade of brain stem gap junctions increases phrenic burst frequency and reduces phrenic burst synchronisation in adult rat. *Journal of neurophysiology* **89**, 135-149.
- Spray DC, Moreno AP, Kessler JA & Dermietzel R. (1991). Characterization of gap junctions between cultured leptomeningeal cells. *Brain Res* **568**, 1-14.
- Stout C, Goodenough DA & Paul DL. (2004). Connexins: functions without junctions. *Curr Opin Cell Biol* **16**, 507-512.
- Stout CE, Costantin JL, Naus CC & Charles AC. (2002). Intercellular calcium signaling in astrocytes via ATP release through connexin hemichannels. *J Biol Chem* **277**, 10482-10488.
- Tirion MM. (1996). Large Amplitude Elastic Motions in Proteins from a Single-Parameter, Atomic Analysis. *Physical review letters* **77**, 1905-1908.
- Valadie H, Lacapre JJ, Sanejouand YH & Etchebest C. (2003). Dynamical properties of the Mscl of Escherichia coli: a normal mode analysis. *J Mol Biol* **332**, 657-674.
- Valdez Capuccino JM, Chatterjee P, Garcia IE, Botello-Smith WM, Zhang H, Harris AL, Luo Y & Contreras JE. (2019). The connexin26 human mutation N14K disrupts cytosolic intersubunit interactions and promotes channel opening. *J Gen Physiol* **151**, 328-341.
- Wangemann P. (2006). Supporting sensory transduction: cochlear fluid homeostasis and the endocochlear potential. *J Physiol* **576**, 11-21.
- Weissman TA, Riquelme PA, Ivic L, Flint AC & Kriegstein AR. (2004). Calcium waves propagate through radial glial cells and modulate proliferation in the developing neocortex. *Neuron* **43**, 647-661.
- Young KC & Peracchia C. (2004). Opposite Cx32 and Cx26 voltage-gating response to CO₂ reflects opposite voltage-gating polarity. *J Membr Biol* **202**, 161-170.
- Yu J, Bippes CA, Hand GM, Muller DJ & Sosinsky GE. (2007). Aminosulfonate modulated pH-induced conformational changes in connexin26 hemichannels. *J Biol Chem* **282**, 8895-8904.
- Zhang Y & Hao H. (2013). Conserved glycine at position 45 of major cochlear connexins constitutes a vital component of the Ca²⁺(+) sensor for gating of gap junction hemichannels. *Biochem Biophys Res Commun* **436**, 424-429.
- Zhao HB. (2017). Hypothesis of K⁺-Recycling Defect Is Not a Primary Deafness Mechanism for Cx26 (GJB2) Deficiency. *Frontiers in molecular neuroscience* **10**, 162.
- Zheng W & Auerbach A. (2011). Decrypting the Sequence of Structural Events during the Gating Transition of Pentameric Ligand-Gated Ion Channels Based on an Interpolated Elastic Network Model. *PLOS Computational Biology* **7**, e1001046.

Figures and Legends

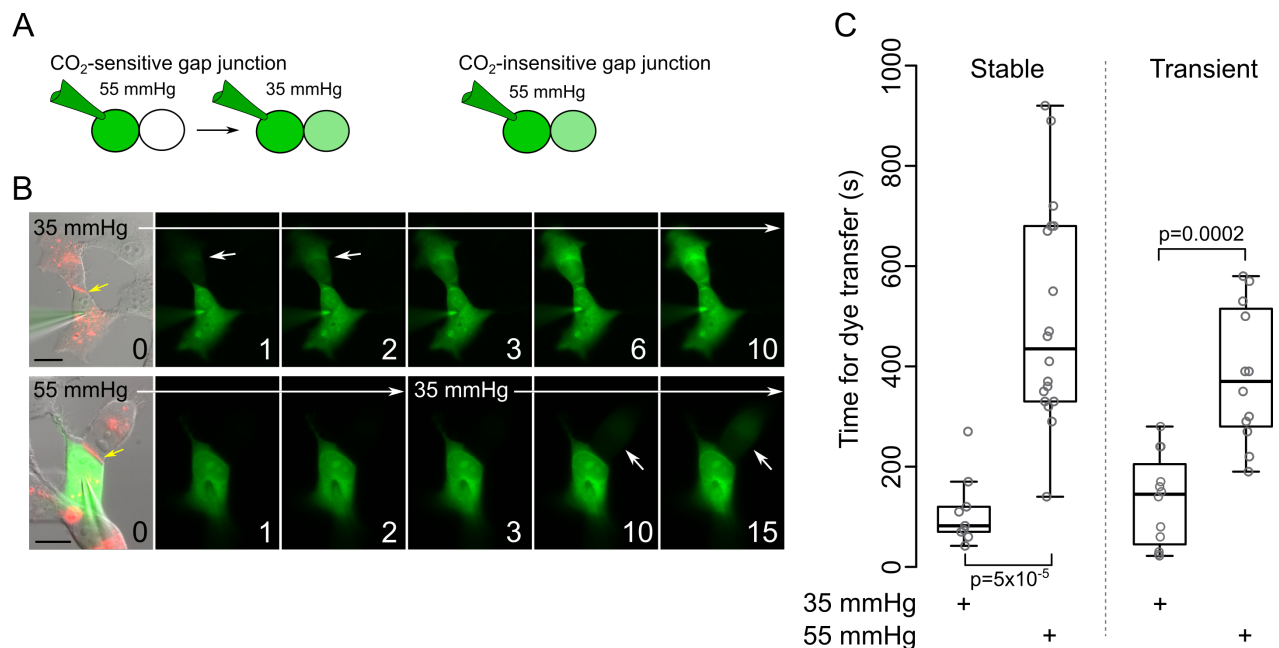


Figure 1. Dye transfer assay to assess the CO₂ sensitivity of gap junction coupling. A) Logic of the assay: a CO₂ sensitive gap junction will display no or very little dye transfer from the donor to acceptor cell under conditions of high PCO₂. This will occur once the cells are transferred to a low PCO₂ saline. A CO₂ insensitive gap junction will exhibit equally rapid dye transfer at low and high PCO₂. B) Images showing dye transfer between coupled cells at two different levels of PCO₂. Numbers in lower right corner are recording time in minutes. Picture at 0 minutes in both rows is a merge of DIC and mCherry (for Cx26, red) and NBDG fluorescence (green) and is the beginning of the recording. The gap junction can be observed as a red stripe between the coupled cells (yellow arrows, both rows). Subsequent pictures show just the NBDG fluorescence. In 35 mmHg PCO₂ dye transfer to the acceptor cell is evident after 1 minute (white arrows). Starting the recording at a PCO₂ of 55 mmHg, and then transferring to 35 mmHg saline after 2 minutes greatly slows dye transfer; fluorescence in the acceptor cell is only seen after 10 minutes (white arrows). Scale bar is 20 μm. C) Summary data for stably expressing (mouse Cx26, *n*=9 and 18 for low and high CO₂ respectively) and transiently transfected (human Cx26, tagged with mCherry, *n*=12 for low and high CO₂) HeLa cells, showing the time for dye in the acceptor cell to reach 10% of the donor starting in 35 mmHg, and starting in 55 mmHg but transferring to 35mmHg after two minutes. When the recordings are commenced in 55 mmHg the dyes transfer time is much longer. Statistical comparisons Mann Whitney U test.

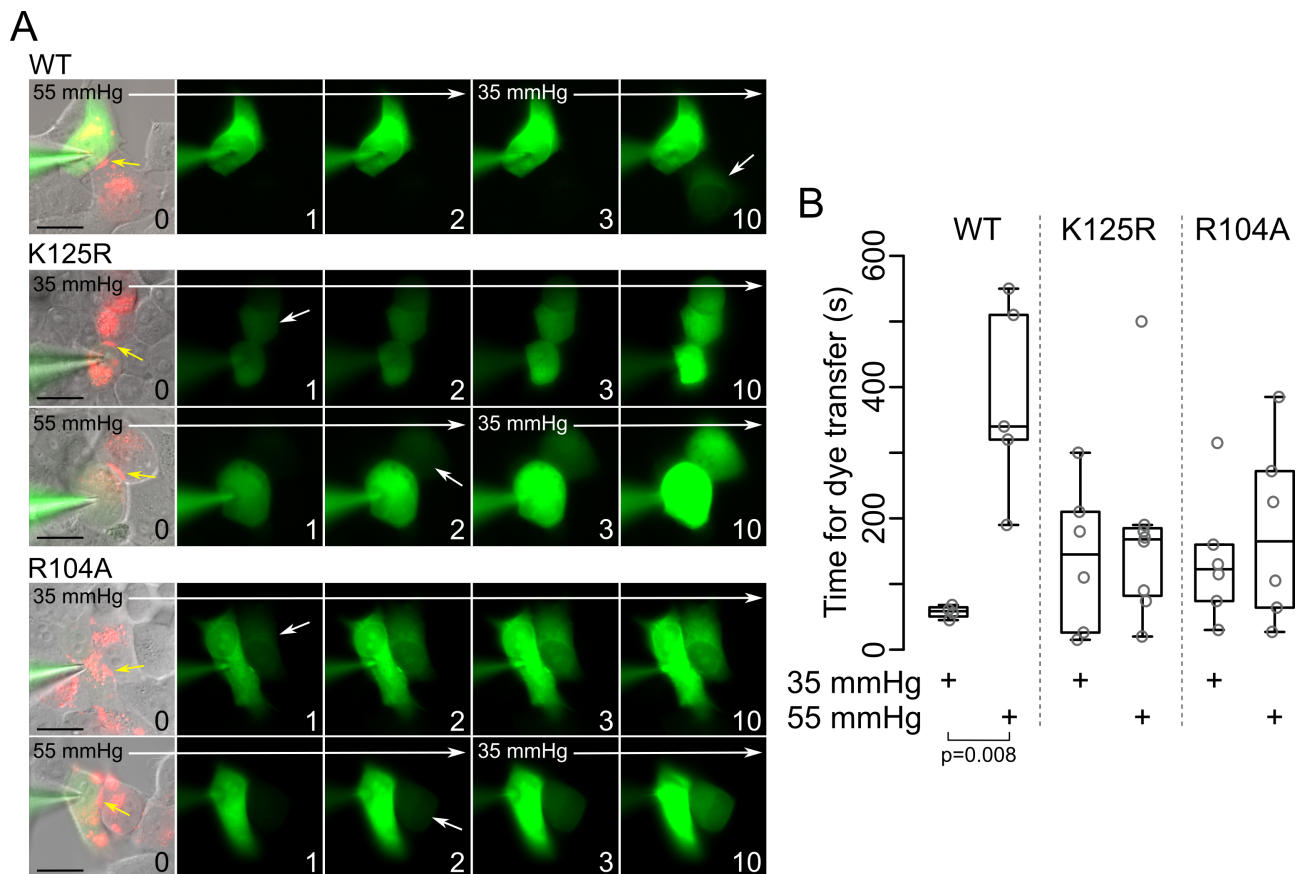


Figure 2. CO₂ dependence of Cx26 gap junction closing depends on the carbamylation motif.

A) Images showing permeation of NBDG through Cx26^{WT}, Cx26^{K125R} or Cx26^{R104A} at different levels of PCO₂. Unlike the Cx26^{WT}, where elevated PCO₂ slows permeation of NBDG to the coupled cell, permeation of NBDG between cells coupled by Cx26^{K125R} or Cx26^{R104A} and apparently unaffected by PCO₂. White arrows indicate appearance of NBDG in the coupled cell, yellow arrows highlight the gap junction structure, scale bar represents 20 μm, numbers in bottom right corners indicate time of image in minutes after start of recording. B) Summary data shows that rat Cx26^{WT} gap junctions are CO₂ sensitive (55 mmHg PCO₂ delays the passage of dye across the gap junction), but those comprised of rat Cx26^{K125R} or rat Cx26^{R104A} show no CO₂-dependence in the time required for dye transfer from the donor to acceptor cell. Mann Whitney U test WT 35mmHg vs WT 55 mmHg, $p=0.008$.

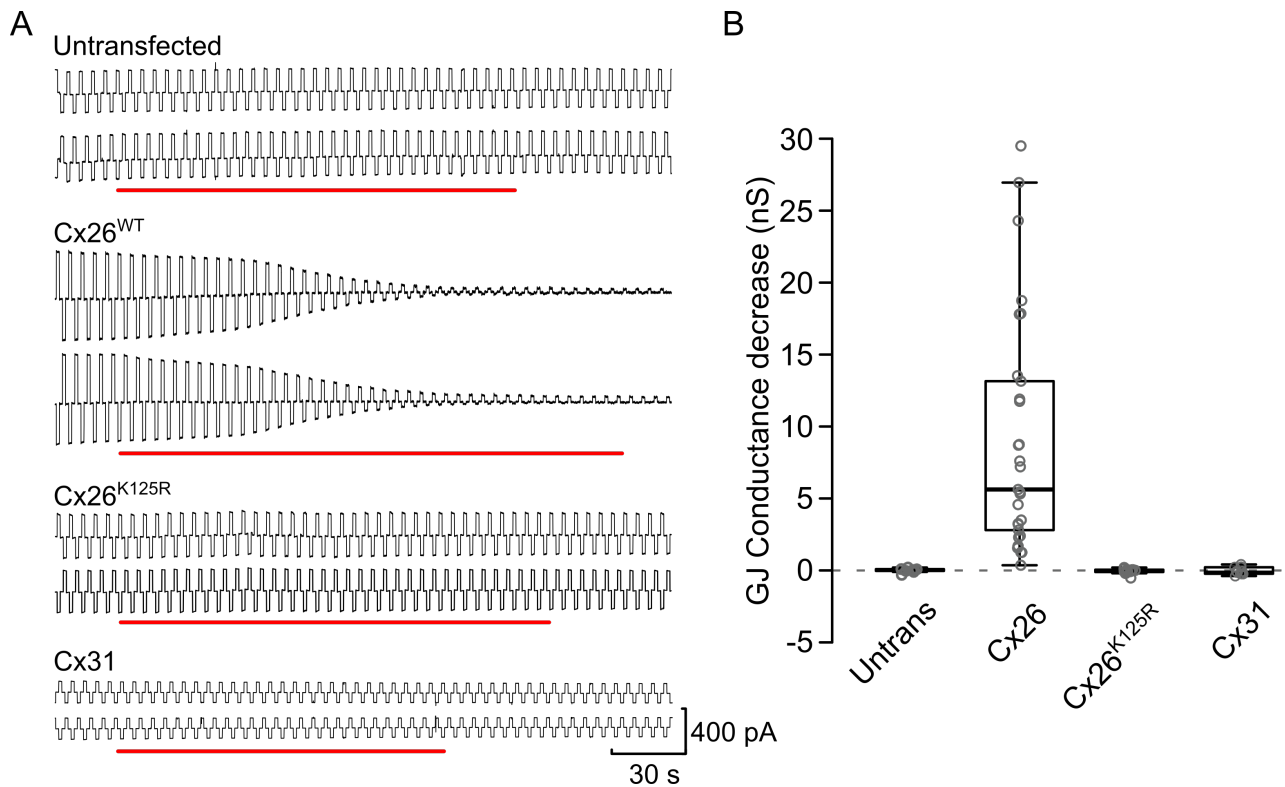


Figure 3. The CO₂-dependent closure of gap junctions is specific to Cx26^{WT}. A) Representative examples of electrophysiological recordings from cells displaying gap junction coupling. In each case, both cells were voltage clamped at -50 mV. On top of the holding potential, alternating +10 mV (1.25 s in duration) steps were applied to each cell. The upward currents represent the whole cell current, which will include the gap junction current; the downward currents represent current flow from the cell at -40 mV to the cell at -50 mV and is thus current flow through the gap junction. Untransfected HeLa cells can exhibit coupling, but this is not sensitive to CO₂. Gap junctions formed between HeLa cells stably expressing mouse Cx26^{WT} are rapidly and completely blocked by CO₂. Gap junctions formed by rat Cx26^{K125R} are unaffected by CO₂, as are rat Cx31 gap junctions. Red bars represent the application of saline with 55 mmHg PCO₂. B) Summary data showing the effect of CO₂ on gap junction coupling between untransfected (parental) HeLa cells, and HeLa cells expressing Cx26^{WT}, Cx26^{K125R} or Cx31.

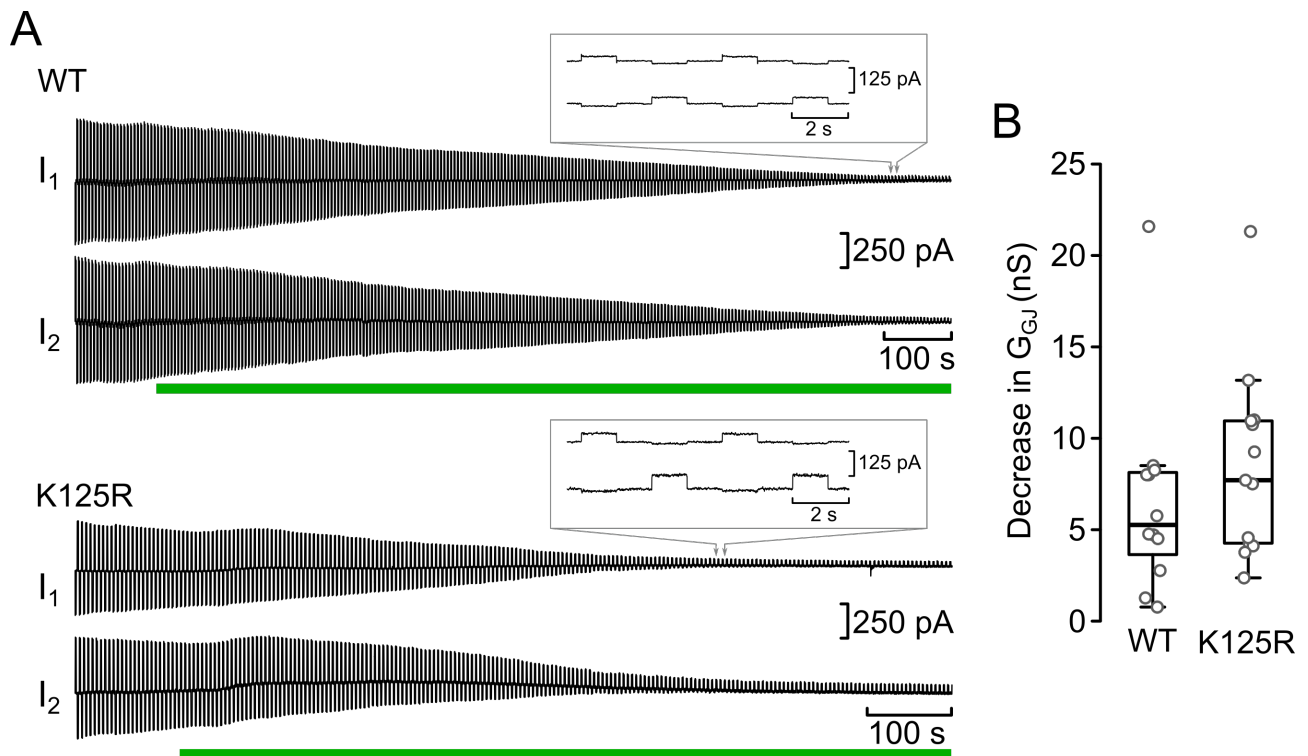


Figure 4. Intracellular acidification closes Cx26 gap junctions and is independent of the carbamylation motif. a) Sample recordings of gap junctions formed between cells transiently expressing human Cx26^{WT} or human Cx26^{K125R} tagged with mCherry. Alternating +10 mV steps were applied to each cell, the downward currents represent the flow of current through the gap junction to the coupled cell. Application of 30 mM propionate (green bar) caused a reduction in the gap junction currents, that was similar for Cx26^{WT} and Cx26^{K125R}. The insets show the current traces at indicated time when Gap junction blockade was almost complete. b) Summary data showing the gap junction conductance decrease caused by acidification of HeLa cells expressing Cx26^{WT} or Cx26^{K125R}.

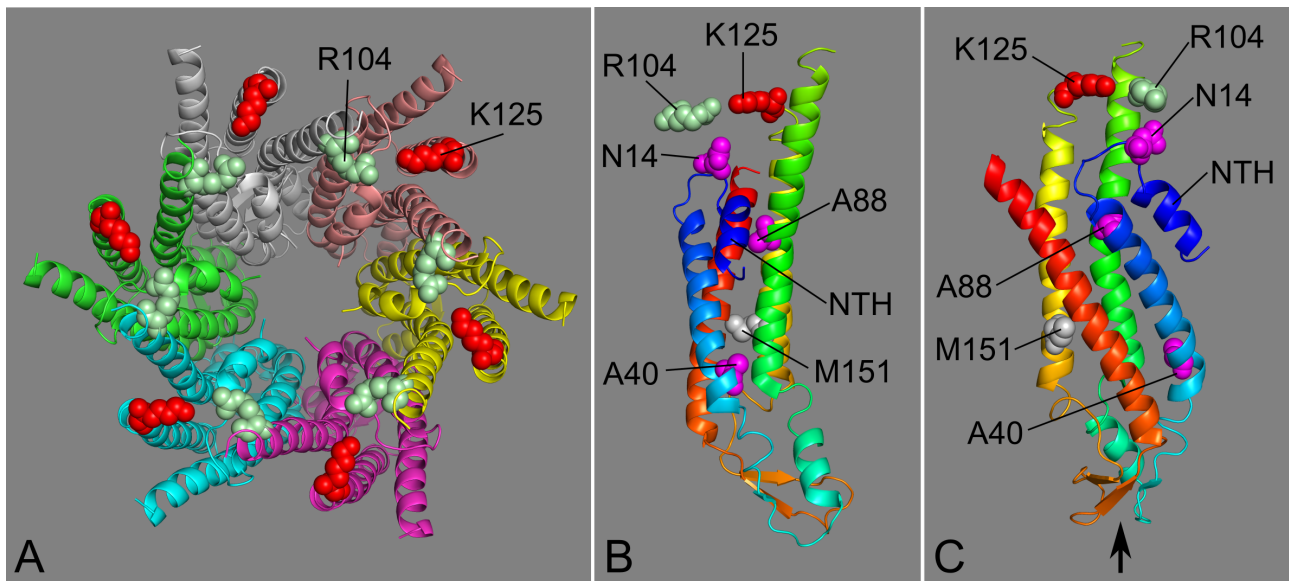


Figure 5. Position of the Cx26 carbamylation motif relative to the KIDS residues mutated in this study. a) View of the hemichannel as seen from the cytoplasmic face. Residues K125 and R104 of the carbamylation motif are shown in red and light green respectively. b) Side view of a single subunit showing the positions of mutated residues (N14, A40 and A88 are mutated in KIDS, M151 was mutated to prevent alternative splicing of KIDS mutated mRNA). R104 from the adjacent subunit is shown aligned to K125 of the subunit. NTH: N terminal helix. c) Additional view of the subunit after rotating it approximately 90° counterclockwise. Arrow indicates the loops in the subunit that dock to a hexamer in an opposed membrane to form a gap junction. Structure based on 2zw3 from the Protein Database.

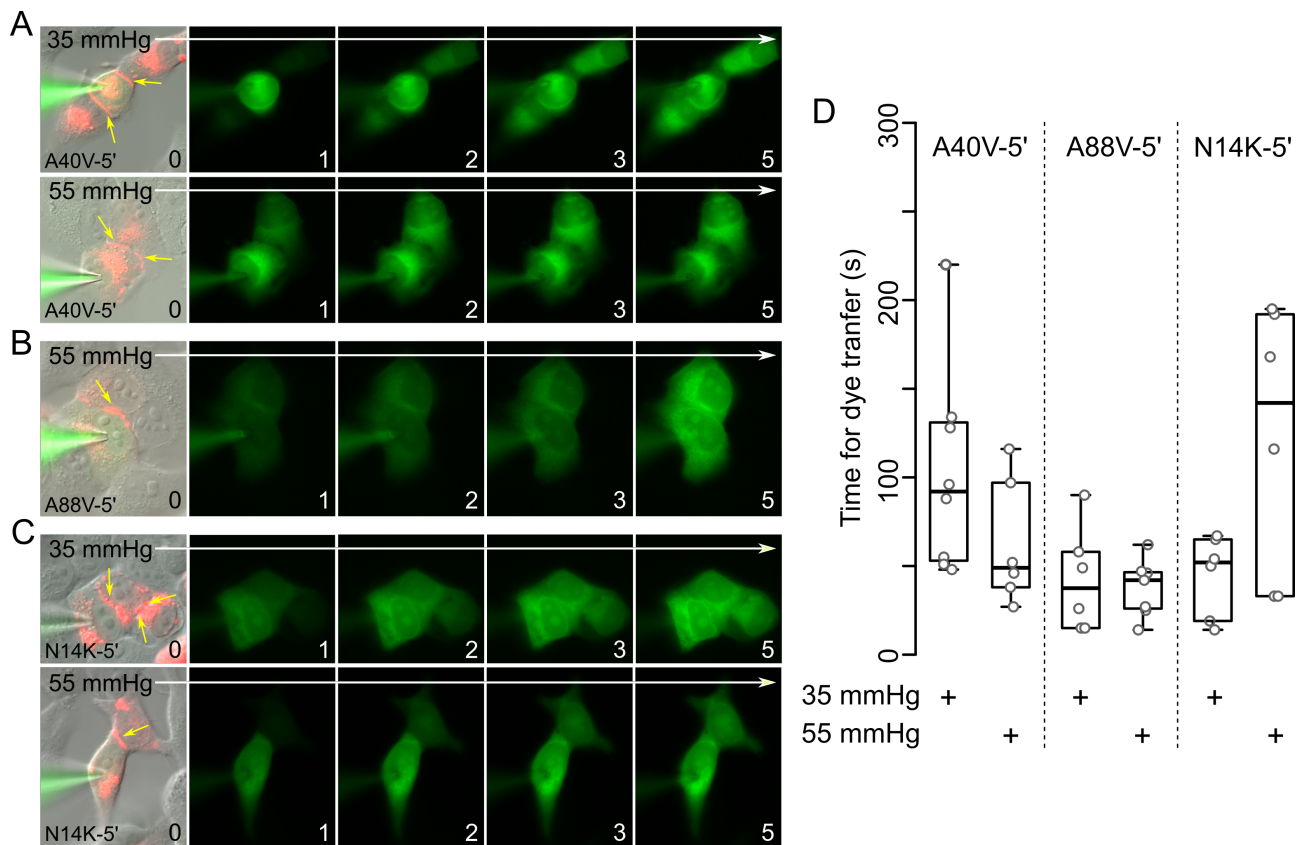
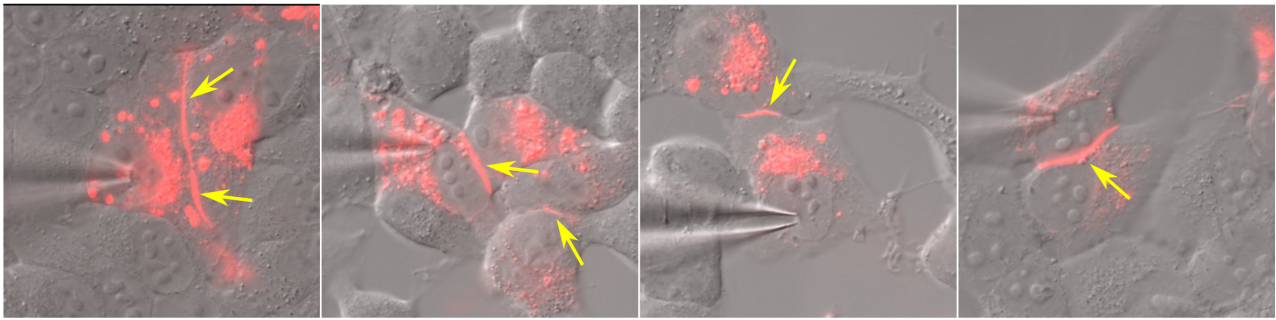


Figure 6. KIDS mutations of human Cx26 alter the CO₂-sensitivity of Cx26 gap junctions. A) Gap junctions (indicated by yellow arrows) formed by Cx26^{A40V-5'} (combining the A40V mutation with M151L, to eliminate alternative splicing) are highly permeable to NBDG and lack any CO₂ sensitivity. The images encompass 5 minutes of recording at a PCO₂ of 35 mmHg (top) and 55 mmHg (bottom). Permeation of NBDG to the coupled cells happens within 2 minutes in both conditions. B) Gap junctions (indicated by yellow arrows) formed by Cx26^{A88V-5'} are insensitive to PCO₂ -rapid permeation occurs to the coupled cell even at a PCO₂ of 55 mmHg. C) Gap junctions formed by Cx26^{N14K-5'} are not closed by CO₂. Permeation of NBDG to coupled cells is shown at PCO₂ of 35 mmHg (top row) and 55 mmHg (bottom row). D) Summary data showing the time for dye transfer to the coupled cell. While A40V-5' and A88V-5' show no difference in permeation time with PCO₂, there is a tendency for the dye to permeate more slowly to the coupled cells for N14K-5'.

A



B

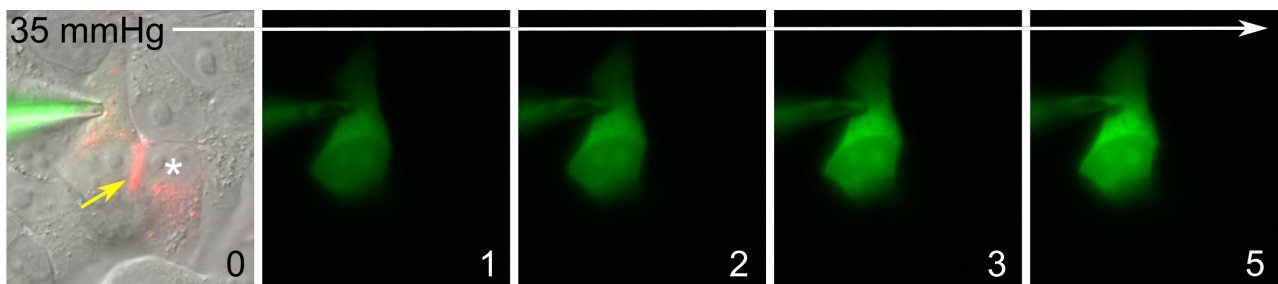


Figure 7. Physical gap junction plaques form between HeLa cells expressing human Cx26^{M151L} tagged with mCherry, but are non-functional. A) The gap junction plaques between cells are indicated by the yellow arrows. For clarity, the green channel (NBDG) has not been merged with the mCherry and DIC images. B) Images of a cell loaded with NBDG that formed a gap junction plaque (yellow arrow) with a neighbouring cell (*). However, NBDG does not permeate to the neighbouring cell within 5 minutes even at a permissive level of PCO₂ (35 mmHg). Numbers represent minutes from start of recording.

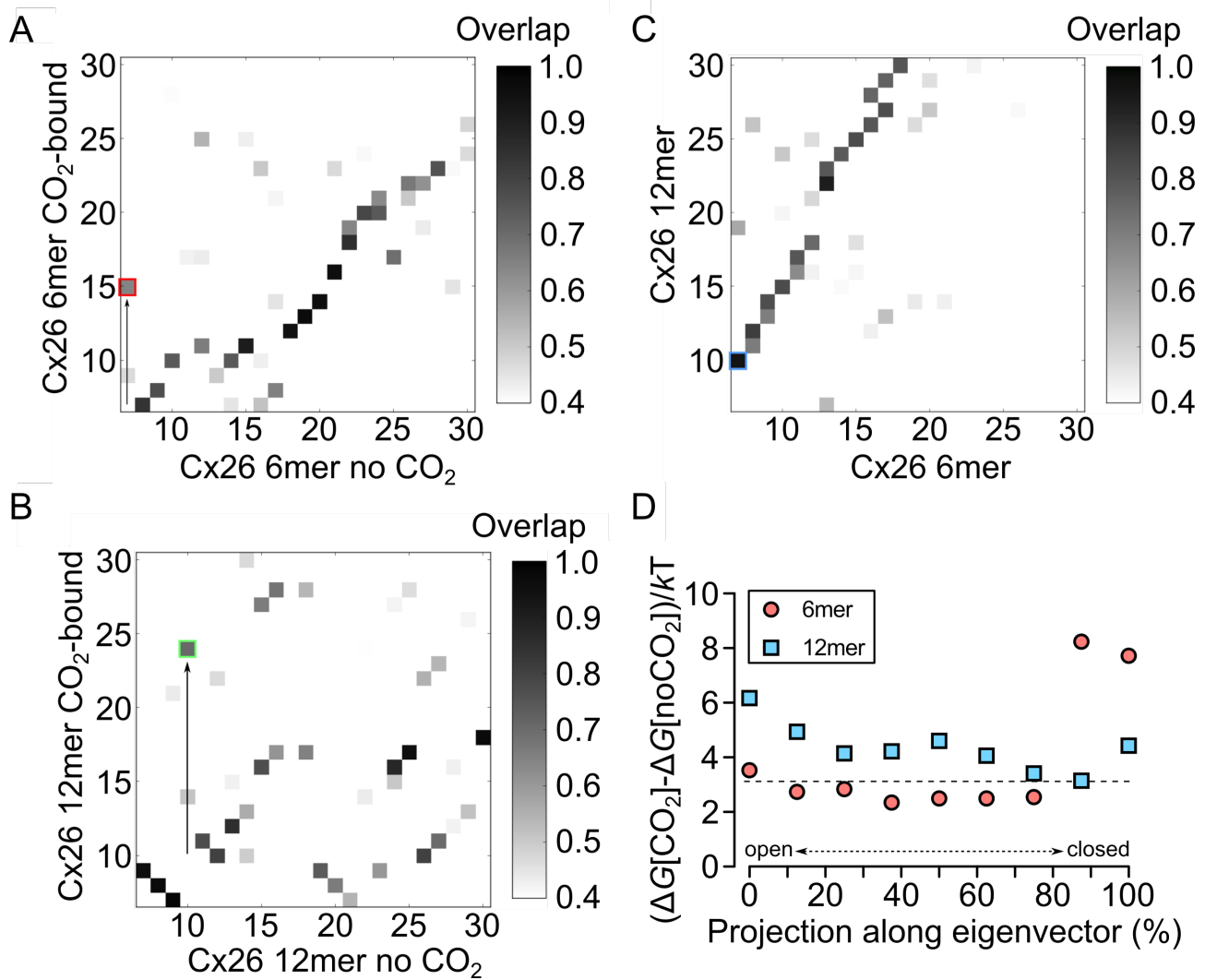


Figure 8. Analysis of the effect of CO₂ on Cx26 hemichannel and gap junction gating via elastic network modelling. a) The main open-close mode in the hemichannel (6mer) in the absence of CO₂ (mode 7) is reordered to mode 15 (red square) in the presence of CO₂. Therefore, this mode contributes less to the total motion of the molecule in the presence of CO₂-the hemichannel spends more time open (Meigh *et al.*, 2013). b) The main open-close mode in the gap junction (12mer) in the absence of CO₂ (mode 10) is reordered to mode 24 (green square) in the presence of CO₂. CO₂ thus reduces the contribution of this mode to the total motion of the molecule, but it is not possible to state whether the gap junction is predominantly in the closed or open state from this analysis alone. c) Correspondence of the modes for the hemichannel (6 mer) and gap junction (12 mer). Mode 7 in the hemichannel corresponds very closely to mode 10 in the gap junction (indicated by blue square). d) For a range of partially open and closed eigenvectors for both the hemichannel and the gap junction, we then calculated the change in free energy on CO₂-binding and thus the influence of CO₂ on the open/closed eigenvector. The closer the free energy value is to zero, the less energy needed to bind CO₂. The x-axis represents trajectory along the open/closed eigenvector going from

fully open to fully closed. The y -axis represents the free energy for binding CO_2 where the higher the value the less preferable is CO_2 -binding. For the hemichannel, CO_2 -binding is less energetically favourable in the closed state, whereas for the gap junction CO_2 -binding is favoured in the closed state.